Electromechanical Properties of Poly(vinylidene fluoride-trifluoroethylene) Networks

R. CASALINI,[1] C. M. ROLAND[2]

[1]Chemistry Department, George Mason University, Fairfax, Virginia 22030

[2]Chemistry Division, Naval Research Laboratory, Code 6120, Washington, DC 20375-5342

Received 25 January 2002; accepted 21 June 2002

ABSTRACT: Random copolymers of 65% vinylidene fluoride and 35% trifluoroethylene were reacted with an organic peroxide, in combination with a free-radical trap, to yield networks of high crosslink density. Crystallization subsequent to the crosslinking yielded ferroelectric materials exhibiting large electrostrictive strains. The magnitude of the electromechanical response increased with an increasing degree of crosslinking, even though this reduced the crystallinity. For the most crosslinked sample, longitudinal (thickness) strains as high as 12% were induced at an electric field of 9 MV/m. This electrostrictive performance exceeded that obtained to date with any poly(vinylidene fluoride) material. © 2002 Wiley Periodicals, Inc. J Polym Sci Part B: Polym Phys 40: 1975–1984, 2002

Keywords: poly(vinylidene fluoride); crystallization; crosslinking; electrostriction; strain

INTRODUCTION

A piezoelectric material undergoes mechanical deformation when an external field is applied, or, conversely, a mechanical stress will cause the surface to develop an effective charge. This phenomenon is attributed classically to a change in the internal polarization induced in crystals lacking a center of symmetry.[1] When no external forces are present, the center of the negative and positive charges will coincide, and there is no net polarization. The application of a mechanical strain or an external field displaces the charges, creating in the first case a dipole moment and consequent surface charge or, in the second case, a change in the crystal dimensions with consequent mechanical strain. For the majority of electromechanically active materials, the dependence of the strain on the electric field is more complicated than the simple linear proportionality expected for piezoelectricity. Electrostriction refers to the quadratic term in the material response.

Piezoelectricity and electrostriction are exploited in various low-power devices, such as sensors, actuators, and sonic transducers. Although ceramics are the dominant materials for such applications, there is great interest in developing electroactive polymers because of their superior processability, toughness and lighter weight (which is especially important for aviation applications). The most promising candidates are copolymers of poly(vinylidene fluoride) (PVDF). In addition to existing commercial usage, PVDF materials with enhanced electromechanical properties are being developed.[2–4]

Recently we reported[5] results for a poly(vinylidene fluoride-trifluoroethylene) [P(VDF-TrFE)] network produced by chemical crosslinking above the crystalline melting point followed by crystal-

Correspondence to: C. M. Roland (E-mail: mike.roland@nrl.navy.mil)

Journal of Polymer Science: Part B: Polymer Physics, Vol. 40, 1975–1984 (2002)

lization. The resulting ferroelectric, semicrystalline material exhibited a high electrostrictive response, with longitudinal strains 20 times larger than the best results reported to date on any PVDF material. Here we describe a systematic study of the thermal and electromechanical properties and their relationship to network chain density.

EXPERIMENTAL

The random copolymer P(VDF-TrFE) (65/35; Solvay, Inc.) was dissolved in *N,N*-dimethylformamide (DMF) along with dicumyl peroxide (DCP; Vanderbilt) and the coagent trimethallyl isocyanurate (TMIC; DuPont). The quantities of DCP and TMIC were kept equal, varying between 5 and 9% by weight in the polymer. The use of TMIC allowed higher degrees of crosslinking to be achieved than the use of peroxide alone. These materials had a crosslink density 20 times greater than that previously obtained chemically[6] and equal to the densities of the most crosslinked networks achieved by electron irradiation.[2]

Films were cast from 10 wt % DMF solutions and were dried initially at 40 °C and then at room temperature for several days *in vacuo*. Curing was carried out at 180 °C for 40 min under moderate pressure with a Carver press. After curing, the film was removed from the press and allowed to cool in ambient air. Note that for some PVDF materials, the electromechanical properties are sensitive to the thermal history.[3,7] Crosslink densities were measured from equilibrium swelling in DMF with a solvent interaction parameter determined previously.[6] Films were placed in an excess of the solvent (at least 50 times the film volume) and allowed to equilibrate for at least a week, with daily replacement of the solvent. Film thicknesses were measured with a micrometer (1-μm resolution). The typical thickness was 75 μm.

For electrostrictive measurements, samples were placed between gold-coated electrodes [see the inset in Fig. 4 (shown later)], with the voltage applied by a waveform generator (Solartron 1254) in combination with a high-voltage amplifier (Trek 610D). The nominal pressure on the sample film was 1.6 kPa because of the upper electrode plate. The effect of such a constraint on the displacement measurements is discussed later. For the results reported here, changes in the film thickness 60 s after the application of the field were determined with an MTI-1000 Fotonic sensor calibrated with a micrometer. The absolute error in these measurements was estimated to be about 8%. The configuration enabled the simultaneous measurement of the displacement by a capacitance method; there is good agreement between the two methods, as previously reported.[5]

The use of the Fotonic sensor allowed measurements of the displacement to be made at various locations on the film surface (over a region of about 10^{-2} cm^2) so that the uniformity of the response could be verified. For measurements of the displacement (at a fixed value of the electric field) with the optical probe at different positions over the top electrode, the standard deviation was 30% of the mean value. The strain measurement at a fixed location had a standard deviation of 11%.

Isothermal dielectric permittivity at low fields ($<$0.3 MV/m) was measured with an Imass time domain spectrometer (10^{-3} to 10^4 Hz) and an HP4284A LCR meter (2×10^2 to 10^6 Hz). The sample was kept in contact with parallel plate electrodes (diameter = 6.4 mm) with springs. During these measurements, the sample was maintained in a nitrogen atmosphere in a Delta Design oven (temperature control = $\pm$ 0.1 K). Measurements from 298 to 358 K were repeated with samples of different thicknesses to assess for any effect from the interface with the electrode. The measured spectra were found to be independent of the sample thickness.

Thermal analysis was carried out with a PerkinElmer DSC-7, with a 10 °C/min rate for both heating and cooling. The sample mass was typically 5 mg.

Mechanical data were acquired on a modified IMass Dynastat mechanical spectrometer. Specimens on the order of 0.15 mm $\times$ 0.29 mm^2 were glued to the test fixtures. A static load was applied, equal to roughly twice the dynamic amplitude.

RESULTS AND DISCUSSION

Swelling Measurements

For each sample the number density of network chains (υ) was calculated from the volume fraction of the network at equilibrium swelling (ν_R):[8]

$$\upsilon = -[\ln(1 - \nu_r) + \nu_r + \chi\nu_r^2]/[V_s(\nu_r^{1/3} - 2\nu_r/f)] \quad (1)$$

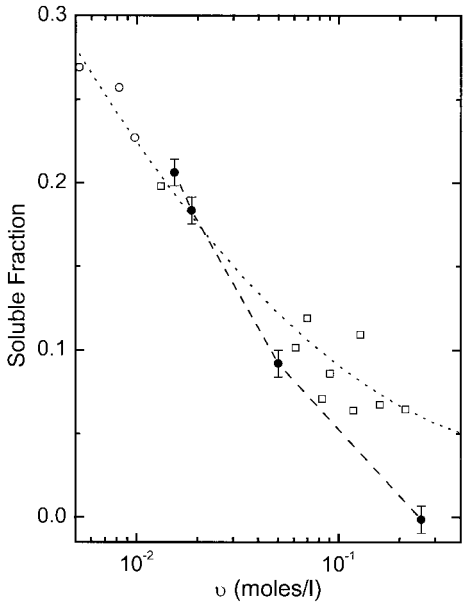

Figure 1. Soluble fraction of P(VDF-TrFE) networks as a function of network chain density. The solid symbols represent networks prepared with DCP and TMIC. The open circles represent crosslinking with only the peroxide, whereas the open squares indicate networks prepared by electron irradiation. These latter two sets of data were taken from ref. 6. A higher soluble fraction implies more chain scission accompanying the crosslinking.

The molar volume of the DMF solvent was V_s = 76.9 mL/mol. For the polymer–solvent interaction parameter, we used $\chi = 0.44$,[6] as determined with the multiple solvent method of Hayes.[9] The functionality of the crosslinks (f) was taken to be 6, which assumes that TMIC is incorporated as the network junction[10,11] and that the reaction with the polymer is complete. Higher concentrations of the DCP and coagent produced a systematic increase of the crosslinking density, up to ν = 0.26 mol/L for 10% each of DCP and TMIC.

From the soluble fraction, determined from the weight loss after swelling, we can quantify the degree of chain degradation accompanying crosslinking. Below the gel point, main-chain scission causes changes in the molecular weight distribution, whereas beyond the gel point, it governs the soluble fraction of the network. Of course, if the rate of chain scission is greater than the rate of crosslink formation, no network is formed. In Figure 1, we have plotted the soluble fraction measured for the networks prepared, along with previous data[6] obtained on electron-irradiated networks.[12] At equal crosslink densities, there is less soluble polymer for the former; that is, chemical crosslinking is associated with less chain degradation. Indeed, at the highest degree of crosslinking, the soluble fraction of the chemically crosslinked network becomes negligible.

Calorimetry

In Figure 2 are shown DSC data for the uncrosslinked, precursor polymer and three networks. The data were acquired during heating at 10 °C/min, following cooling from above the melting point at 10 °C/min. For the highest degree of crosslinking, there is a reduction by roughly half in the extent of crystallinity, along with a 17 °C decrease in the melting temperature.

At lower temperatures, we observe the Curie transition, which indicates that the P(VDF-TrFE) networks retain the ferroelectric character of the uncrosslinked polymer. The Curie temperature (T_c) in Figure 2 is essentially unchanged by crosslinking, although its magnitude decreases in

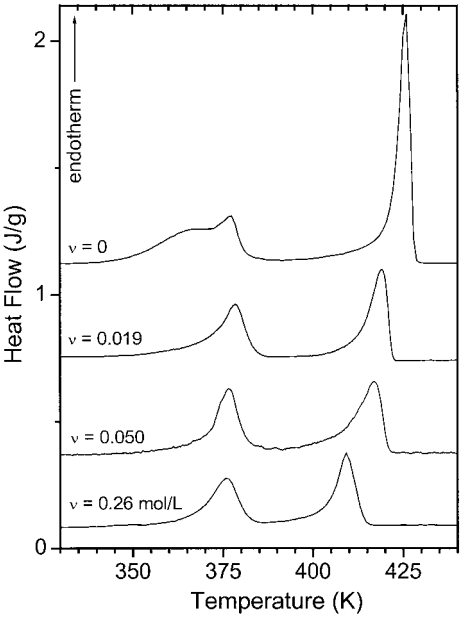

Figure 2. DSC of three networks and the precursor P(VDF-TrFE) obtained during heating from room temperature at 10 °C/min. The network chain densities are indicated. Note that crosslinking has only a modest effect on the Curie transition (ca. 378 K). The degree of crystallinity is reduced to roughly one-third for the highest crosslinking level in comparison with the uncrosslinked copolymer. Despite the high level of crosslinking, there is only a 17 °C suppression of the melting point.

proportion to the degree of crosslinking. It is evident from Figure 2 that the peak associated with the Curie transition is altered by crosslinking. For the uncrosslinked copolymer, two Curie transition peaks are observed, a broad one at a lower temperature and a narrow one at a higher temperature. However, for the networks, there is only a single transition, quite similar to the higher temperature peak observed for the uncrosslinked copolymer.

In an earlier study[13] of the Curie transition for the uncrosslinked copolymer (65/35) crystallized under different conditions, the appearance of two peaks was interpreted to be due to the coexistence of two ferroelectric phases. The higher temperature peak was identified as a more ordered phase. From this, we conclude that in the copolymer network, the formation of the less ordered ferroelectric phase is hindered by the crosslinking process. The direct identification of the remaining phase and an understanding of its role in the unusual electrostrictive properties of the copolymer networks is currently under investigation.

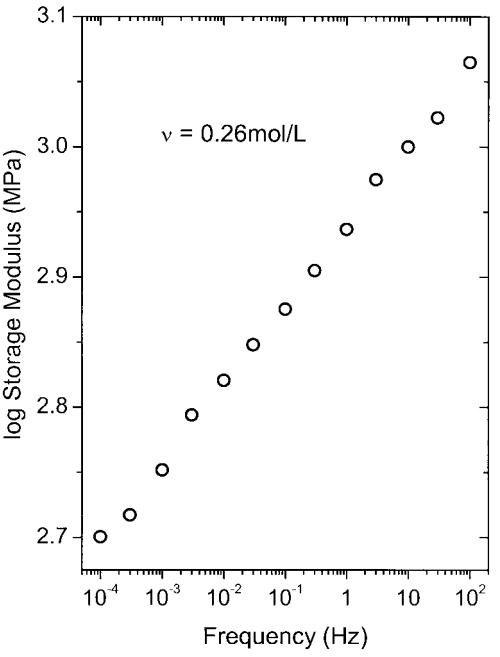

Figure 3. Dynamic mechanical storage modulus at room temperature for the copolymer network with the highest crosslink density. Over this range of frequencies, the loss tangent was essentially constant (0.11 ± 0.2).

Mechanical Measurements

The dynamic modulus for the most crosslinked network was measured to be 0.5–1.1 GPa, depending on the frequency (Fig. 3). Over the range of 10^{-4} to 10^{2} Hz, which at room temperature corresponds to the rubbery plateau region of the viscoelastic spectrum, the loss tangent was 11% ± 0.2. The high modulus of the networks reflects their retention of a high degree of crystallinity. Because deformation of the crystal domains per se is negligible, the stress is concentrated in the surrounding amorphous phase. This amplifies the modulus, which otherwise would be very low (~1MPa).[14,15] Moreover, a reduction in the crystallite size increases the specific surface area of the crystalline phase, with a more effective enhancement of the modulus.[16] This may account for the retention of a high modulus in the networks, notwithstanding their reduced level of crystallinity.

Strain Measurements

The field dependence of the longitudinal strain induced by an applied field, determined with both the optical and capacitance methods, was reported previously[5] for the most crosslinked network herein. Here we compare the longitudinal strain (the relative change in thickness) for networks of different crosslink densities, with the aim of better understanding the process.

The crosslink density dependence of the longitudinal strain, measured under a static field of 9 MV/m, is shown in Figure 4. There is a monotonic increase in the electromechanical response with the degree of crosslinking, with a strain of 12% attained for the network with ν = 0.26 mol/L. Notwithstanding the low value of the electric field, these strains greatly exceed anything obtained to date with PVDF-type materials (see Table 1). Moreover, because electrostriction varies quadratically with the field (except at very high fields[17]), better results may be achievable. Currently, we are limited by electrical breakdown related to electrode edge effects and film quality. Postcuring for the removal of small-molecule byproducts of the curing process may improve this aspect of the performance.

The origin of this high electrostrictive response is not entirely understood. For the electron-beam-irradiated PVDF copolymer, the electrostrictive strain has been ascribed[2] to a change in lattice dimensions resulting from a field-induced change from the nonpolar α phase to the ferroelectric β-crystalline form. However, the crystal dimen-

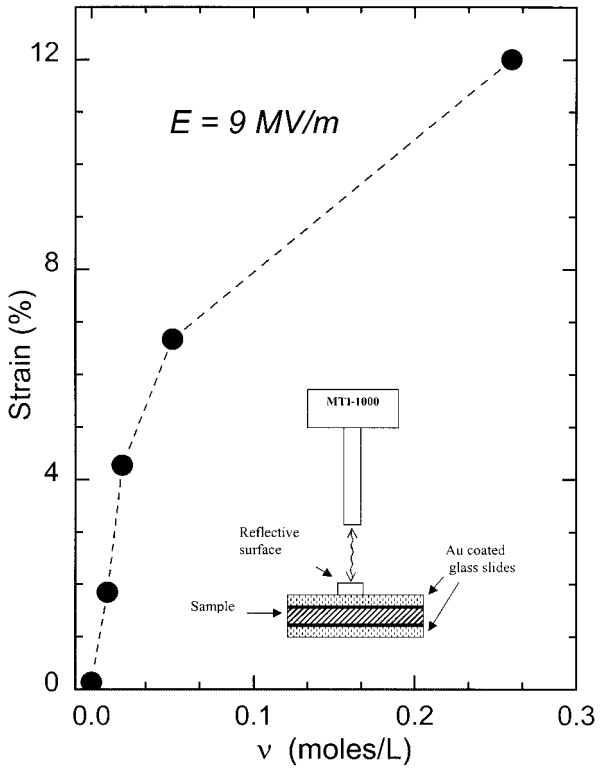

Figure 4. Longitudinal (thickness) strain induced in PVDF copolymer networks of various crosslink densities. The magnitude of the electric field is indicated. The inset shows the setup used to measure the strain.

sion in PVDF decreases at most 10% (the *b* axis of the unit cell),[18] which imposes an upper bound on the electrostrictive response available from such a mechanism. Moreover, there is a concomitant increase in the *c* axis (chain direction),[18] so that in the absence of orientation, the macroscopic dimensional changes accompanying an α- to β-crystal phase change would appear to be rather small.

However, large strains (as much as 6%) have been observed in unoriented vinylidene fluoride copolymers that are ferroelectric[3] (β phase existent in the absence of a field), indicating that mechanisms other than the phase-change model proposed by Zhang et al.[2] must be operative. For example, the role played by the coexisting amorphous material (characterized by very different mechanical and electrical properties) must be assessed. It is evident that the manner in which electrical forces act on the crystals embedded in an amorphous phase is quite different (and more efficient[19]) than the action of mechanical forces. Any contribution herein from bound charges,[20] as exploited with electrostrictive polyurethanes,[21] is unknown, although measurements at higher frequencies may be revealing. In fact, a model involving mobile charges that screen the internal field has been proposed as a possible mechanism for the large electrostrictive strains in irradiated PVDF copolymers.[22,23]

We also consider the possibility that in a material composed of two phases (amorphous and crystalline) with very different conductivities, free ionic charges will give rise to a Maxwell–Wagner polarization.[24,25] The application of an electric field induces a current (because of the drift of ions within the material), with consequent polarization due to a discontinuity in the charge carrier concentration at the interfacial regions. Given the finite diffusion time of the charges, this phenomenon will be manifested as a dielectric relaxation, with the shape and intensity directly related to the electrical properties and spatial distribution of the two phases.

The principal methods used to date to achieve better electromechanical properties in PVDF materials are listed in Table 1. These include electron-beam irradiation,[2] rapid quenching from the melt,[3,26] and incorporation into the polymer backbone of a third monomer.[4] For a better comparison of the performances, we estimated values for the electrostrictive coefficient, defined as $M = s/E^2$.[27] The common feature of these disparate approaches is a reduction of the crystallite size, either by the introduction of defects (radiation-induced or from chain units unaccommodated by the crystal unit cell), or kinetically via quenching.

Table 1. Electromechanical Properties of Polyvinylidene Copolymers and Terpolymers

Material[a]	Strain (at Field)	M	Reference
Electron-irradiated P(VDF-TrFE)	4.2% (150 MV/m)	1.9×10^{-6}	2
Quenched P(VDF-HFP)	4% (60 MV/m)	1.1×10^{-5}	3
P(VDF-TrFE-HFP)	2.5% (50 MV/m)	1.0×10^{-5}	4
Chemically crosslinked P(VDF-TrFE)	12% (9 MV/m)	1.5×10^{-3}	This work

[a] HFP = hexafluoropropylene.

Smaller polar domains are more effectively oriented by an applied field. Moreover, at a sufficiently small crystallite size, the orientation of the crystallite per se, rather than mere rotation of atoms within the crystallite, becomes possible, enabling higher strains to be attained. In a similar fashion, chemical crosslinks yield small crystallites by precluding chain units adjacent to the junctions from incorporating into the lamella.[28,29]

Our chemical crosslinking has similarities to the effect of electron radiation, both yielding networks of comparable crosslink density.[6] However, these materials exhibit a Curie transition above room temperature (Fig. 2); that is, the ferroelectric phase of the precursor copolymer is retained. T_c of the uncrosslinked copolymer is governed by the concentration of the trifluoroethylene (TrFE) comonomer. The normal phase of unstretched PVDF homopolymer is paraelectric, but at a sufficiently high TrFE content, the copolymer becomes ferroelectric.[30–33] Ionizing radiation entails substantial side reactions (isomerization, cyclization, and chain scission) that change the molecular structure of PVDF.[34–37] One result is the transformation of the P(VDF-TrFE) copolymer into a paraelectric material.[38] As seen in Figure 1, chemical crosslinking occasions less degradation of the P(VDF-TrFE), and so the ferroelectric character is preserved.

Sources of Error in Strain Measurements

In light of the extraordinary strain levels achieved, a discussion of the various errors that may affect the strain measurements is appropriate. An obvious source of error would be any out-of-plane motion of the film during the strain measurements. To investigate any influence from such bending, we obtained results for a film 4.5 times thicker than the sample (ν = 0.26 mol/L) in Figure 4, that was prepared under the same conditions (longitudinal dimension = 340 ± 15 μm). Because the out-of-plane stiffness is proportional to the third power of thickness, the resistance to bending will be 2 orders of magnitude larger for this thicker film. Nevertheless, under the same electric field, the strain, albeit lower, was within 50% of that of the thinner (75 μm) film. This difference, far smaller than expected for bending, can be otherwise explained by differences in the thermal history and crosslink density.

An obvious way to ensure that the film remains flat is to apply pressure to the upper surface. For the data in Figure 4, the pressure due to the weight of the upper electrode (a metalized glass plate) was 1.6 kPa. If this pressure is too large, however, longitudinal displacement of the film will be reduced because of the constraint of the lateral motion necessary to conserve volume. For complete constraint (e.g., perfect adhesion of the film surfaces to the confining plates), the apparent modulus (Y) is[39]

$$Y = Y_0\left(1 + \frac{a^2}{2d^2}\right) \tag{2}$$

where Y_0 is the modulus of the unconstrained material, a is the lateral dimension of the sample, and d is the thickness. For a = 15 mm and d = 75 μm, eq 2 gives $Y = 200Y_0$. Therefore, the application of a normal pressure can severely reduce the obtained strain.

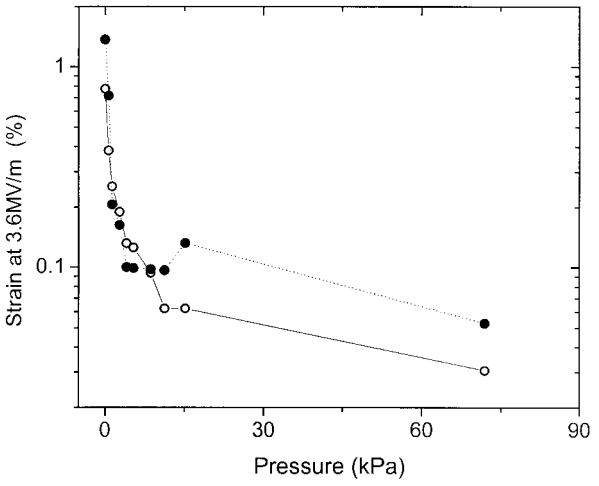

Figure 5. Effect of pressure applied normal to the film on the longitudinal strain measured after the application of an electric field (3.6 MV/m). The pressure was applied by weights being placed on the upper electrode. The two sets of data refer to samples (●) 75 and (○) 340 μm thick.

In Figure 5, we display the static strain after the application of a 3.6 MV/m field, for different pressures applied normal to the strain direction. The two data sets correspond to the two samples of different thicknesses (75 and 340 μm) prepared under the same conditions ($\nu \approx$ 0.26 mol/L). The pressure was applied by dead-weighting of the top plate. Figure 5 shows a rapid decrease in the strain (as much as 1 order of magnitude) for fairly modest pressures. Note that these same pressures would induce mechanical strains of only about 10^{-6}. The effect seen in Figure 5 is not due

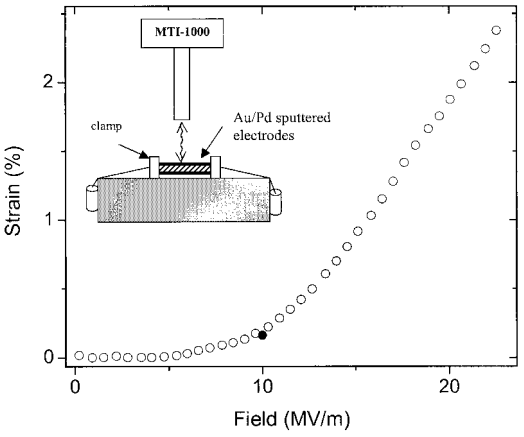

Figure 6. Longitudinal strain versus an applied field measured with (○) the optical method on a film with sputtered electrodes (thickness ~ 50 nm) on both surfaces. The top electrode also served as the reflective surface for the Fotonic sensor. A pair of 100-g weights kept the film flat, as illustrated in the inset. The crosslink density was $\nu = 0.26$ mol/L, and the thickness was 60 μm. A single measurement obtained with (●) the capacitance method is also shown.

to bending (or its suppression), as evidenced by the similar behaviors of the two films. Rather, as suggested by eq 2, thin films subjected to a confining pressure experience a substantial reduction in their deformability. Such an effect has been described previously in the literature.[27,40] Notwithstanding these considerations, it is noteworthy that even with an order of magnitude decrease in the electrostrictive coefficient, the network still exhibits a larger electrostrictive response than has been reported for other PVDF materials (Table 1).

To further investigate the effect of constraints on the film displacement, we used an alternative configuration, with the upper plate removed and replaced by a Au/Pd conductive coating (thickness ~ 50 nm) sputtered directly onto the film. A schematic of this setup is shown in the inset of Figure 6. The film was kept flat by two weights (100 g each) suspended from the ends. The longitudinal strain was then measured at various positions by the optical probe being moved. The standard deviation of these measurements was 30% of the mean value, indicating an absence of bending or significant nonuniformities in the film.

Representative results obtained with this configuration are shown in Figure 6 (open circles) for a sample with a crosslink density of $\nu = 0.08$ mol/L. For comparison, we include a single measurement for the same sample made with the capacitance method (solid circle). There is good agreement between the methods. Note, however, that the strains are lower than those in Figure 4. From Figure 6, we calculate $M = 4.6 \times 10^{-5}$ m^2/MV^2, whereas Figure 4 yields $M = 8 \times 10^{-4}$ m^2/MV^2. The difference between these samples is that only the former has metalized surfaces. Such constraint of the sample displacement due to a metal surface layer has been reported previously[27] and is quite consistent with the effect of pressure seen in Figure 5.

Dielectric Response

Previous dielectric investigations of P(VDF-TrFE) with the same copolymer composition (65/35) identified three dielectric relaxation processes.[41–43] A high-frequency process is observed for $T > T_c$, the strength of which follows the Curie–Weiss law.[41] At T_c, the total dielectric strength shows an anomaly, and there is a crossover to a second process. This α process has a dielectric strength that rapidly decreases with temperature, whereas the temperature dependence of the α-relaxation time is well described by a Vogel–Fulcher–Tamman (VFT) law.[44] At still lower temperatures [especially below the glass-transition temperature (T_g)], a third process (β) with an Arrhenius temperature dependence is observed. The scenario for $T < T_c$ is similar to that for amorphous polymers, in which a cooperative structural relaxation (α) with a VFT behavior markedly slows down in proximity to T_g, whereas a secondary noncooperative relaxation continues to exist both above and below T_g.[45] The maxima of the relaxation peaks for the α and β processes tends to merge at $T = 298$ K at a frequency of $\nu = 10^6$ Hz.[41,43] Therefore, in the room-temperature spectrum, we expect one peak at about 10^6 Hz. As observed by Furukawa et al.[41] in a previous investigation of the P(VDF-TrFE) 65/35 copolymer, there is no separation in time between the respective relaxations of the amorphous and crystalline phases. Only a single process is present (apart from the β relaxation), indicating that the crystalline and noncrystalline motions arise from a common process.

Dielectric spectra for the P(VDF-TrFE) network ($\nu = 0.26$ mol/L) are presented in Figure 7. At room temperature, a decrease in the real part of the permittivity (ϵ') and an increase in the imaginary part (ϵ'') are evident at a higher frequency. This relaxation has a maximum around 10^6 Hz and, on the basis of both its frequency and amplitude, appears to correspond to the α relax-

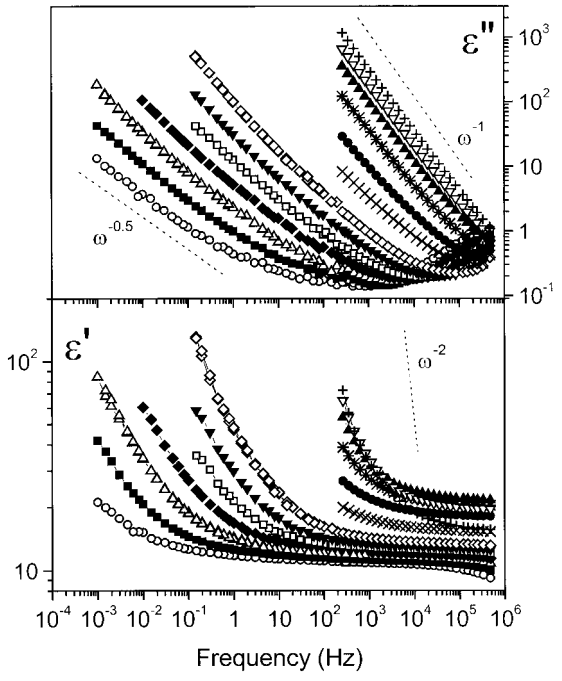

Figure 7. Isothermal measurement of the real (ϵ') and imaginary components (ϵ'') of the dielectric constant versus the frequency for a P(VDF-TrFE) network with crosslink density of $\nu = 0.26$ mol/L. The temperatures of the measurements were (○) 298, (■) 308, (△) 318,, (♦) 328, (□) 338, (▼) 348, (◇) 358, (×) 373, (●) 378, (✱) 383, (▲) 388, (▽) 398, and (+) 408.

ation observed in the uncrosslinked copolymer.[41,43]

In the same spectra at room temperature, at a much lower frequency, an increase in both the real (ϵ') and imaginary (ϵ'') parts of the permittivity can be seen. This is a clear indication of the presence of a second relaxation (α'), with a maximum at a frequency lower than our measurement range. With increasing temperature, the relaxation time of the α' process decreases, but a distinct maximum cannot be observed in the ϵ'' spectra because of presence of the DC conductivity (σ_{DC}). The latter dominates the spectra at high temperatures, contributing to the dielectric loss as a power law: $\epsilon'' = \sigma_{DC}/\epsilon_o\omega$.[45] At high temperatures, the ω^{-2} slope of ϵ' suggests an electrode polarization effect as well.

The distinctive characteristic of these spectra is the presence of the α' relaxation, which is absent in the dielectric spectra of the uncrosslinked copolymer. This α' relaxation has a substantial amplitude, giving rise to a large dielectric constant at a low frequency. The possibility exists that this α' process is related to the electrostrictive response observed in the PVDF networks. However, it is presently unknown to what extent the α' process is related to the presence of ions in the material (i.e., Maxwell-Wagner polarization) or to motion of the crystallites.

In an ideal ferroelectric material at T_c, the crystallites undergo a change of structure, passing from a polar phase (ferroelectric) to a nonpolar phase (paraelectric). Because of the presence of disorder in a real ferroelectric, this transition will occur in a temperature interval near T_c. This change is observed as a change in the temperature dependence of the dielectric strength for processes involving the motion of the crystallites. Moreover, as observed previously for PVDF copolymers, because of thermal hysteresis, the temperature of the Curie transition is affected by thermal history (T_c is lower during cooling than during heating). Accordingly, any contribution to the permittivity from the ferroelectric phase should be different for heating and cooling. In Figure 8 are shown two isochronal measurements at 50 Hz and 2 kHz obtained during heating from 293 to

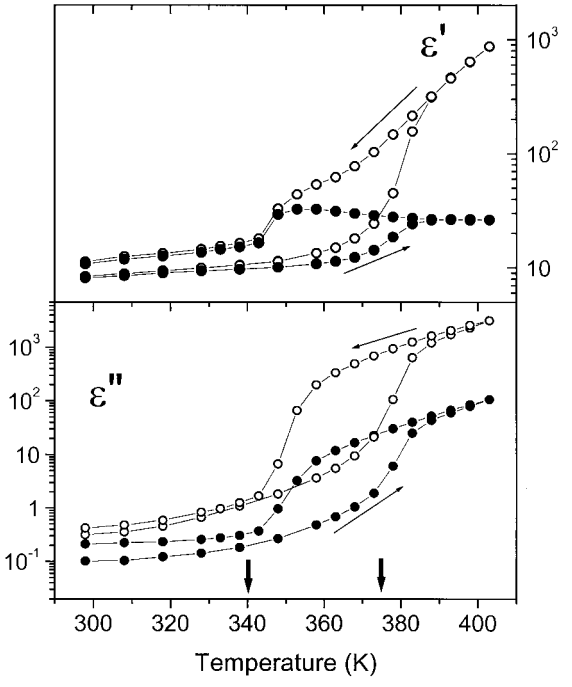

Figure 8. Isochronal measurements of the real (ϵ') and imaginary components (ϵ'') of the dielectric constant versus the frequency for the same sample shown in Figure 7. The frequencies of the measurements were (○) 50 Hz and (●) 2 kHz. The arrows indicate the measurements during heating and cooling. The vertical arrows indicate T_c's measured by DSC during heating (higher value) and cooling at 10 K/min.

403 K, followed by cooling back to 293 K. The respective T_c values determined by DSC during heating and cooling are indicated. The correlation of the behavior of both ϵ' and ϵ'' and the calorimetric T_c implies a connection between the α' relaxation and the ferroelectric crystalline phase. This correlation, along with the high values of the dielectric constant at a low frequency, offers some insight into the origin of the electrostrictive behavior of the PVDF networks.

CONCLUSIONS

The electrostrictive behavior of P(VDF-TrFE) networks of various crosslink densities was investigated. Network formation modifies both the degree of crystallinity and the nature of the ferroelectric phase. Electric-field-induced longitudinal strains for the networks increase with increasing crosslink density.

Dielectric measurements at low electric fields reveal the presence of a relaxation at a low frequency, which was not previously observed in the uncrosslinked copolymer. The properties of this relaxation mode correlate with the crystalline phase. This process could account for the high level of the electrostrictive coefficient measured for the networks. However, the marked decrease in the dielectric constant with frequency implies that the amplitude of the electrostrictive strain should likewise be reduced at a higher frequency. The measurement of the frequency dependence of the electrostrictive strain certainly would be useful. Such work may also guide future modifications for the further improvement of the electromechanical properties.

By virtue of their high mechanical modulus and large electrostrictive response, the P(VDF-TrFE) networks have the potential to extend the range of utility for polymer-based electromechanical materials. Potential fields of application include sonar transducers and loudspeakers, actuators, artificial muscles, robotics, and active controls for optics and vibration constraint systems.

This work was supported by the Office of Naval Research. The authors thank Dr. R. Corsaro and Dr. G. Buckley for their experimental assistance and stimulating discussions.

REFERENCES AND NOTES

1. Ashcroft, N. W.; Mermin, N. D. Solid State Physics; Holt, Rinehart and Winston: New York, 1976.
2. Zhang, Q. M.; Bharti, V.; Zhao, X. Science 1998, 280, 2102.
3. Lu, X.; Schirokauer, A.; Scheinbeim, J. IEEE Trans Ultrason Ferroelectr Freq Control 2000, 47, 1291.
4. Petchsuk, A.; Chung, T. C. Polym Prepr 2000, 41(2), 1558.
5. Casalini, R.; Roland, C. M. Appl Phys Lett 2001, 79, 2627.
6. Buckley, G. S.; Roland, C. M. Appl Phys Lett 2001, 78*, 622*.
7. Elhami, K.; Gauthier-Manuel, B.; Manceau, J. F.; Bastien, F. J Appl Phys 1995, 77, 3987.
8. Flory, P. J. Principles of Polymer Chemistry; Cornell University Press: Ithaca, NY, 1953.
9. Hayes, R. A. Rubber Chem Technol 1986, 59, 138.
10. Apotheker, D.; Finlay, J. B.; Krusic, P. J.; Logothetis, A. L. Rubber Chem Technol 1982, 55, 1004.
11. Logothetis, A. L. Prog Polym Sci 1989, 14, 251.
12. This was supplied by Q. M. Zhang of Penn State University.
13. Tanaka, H.; Yukawa, H.; Nishi, T. Macromolecules 1988, 21, 2469.
14. Peterlin, A. In Ultra High Modulus Polymers; Ciferri, A.; Ward, I. M., Eds.; Applied Science: London, 1979.
15. Peng, K. L.; Roland, C. M. J Polym Sci Part B: Polym Phys 1993, 31, 1339.
16. Medalia, A. J Colloid Interface Sci 1970, 32, 115.
17. Urayama, K.; Kircher, O.; Bohmer, R.; Neher, D. J Appl Phys 1999, 86, 6367.
18. Kepler, R. G.; Anderson, R. A. Adv Phys 1992, 41, 1.
19. For an amorphous material, the mechanical energy associated with electrostrictive strains is the same as that for simple mechanical deformation; both are related to Young's modulus of the material. However, a semicrystalline material is heterogeneous, and so the situation is quite different. Although mechanical strains still involve primarily the motion of the amorphous phase (because its modulus is much lower than that of the crystalline phase), the molecular processes giving rise to deformation induced by an electric field involve displacements within the crystal lattice. Such motion involves much less mechanical energy than would be expected from a consideration of the macroscopic modulus of the material.
20. Sessler, G. M.; Das-Gupta, D. K.; DeReggi, A. S.; Eisenmenger, W.; Furukawa, T.; Giacometti, J. A.; Gerhard-Multhaupt, R. IEEE Trans Electr Insul 1992, 27, 872.
21. Guillot, F. M.; Balizer, E.; Jarzynski, J. Presented at the U.S. Navy Workshop on Acoustic Transduction Materials and Devices, Baltimore, MD, May 14–16, 2001.
22. DeReggi, A. S.; Balizer, E.; Neumann, D. A.; Bateman, F. 2000 Conference on Electrical Insulation

and Dielectric Phenomena; IEEE: Piscataway, NJ, 2000; Vol. 1, p 191.
23. Balizer, E.; DeReggi, A. S.; Neumann, D. A.; Bateman, F. 1999 Conference on Electrical Insulation and Dielectric Phenomena; IEEE: Piscataway, NJ, 1999; Vol. 1, p 104.
24. Maxwell, J. C. A Treatise on Electricity and Magnetism; Dover: New York, 1954.
25. Wagner, K. W. Arch Electrotechnol 1914, 2, 371.
26. Lu, X.; Schirokauer, A.; Scheinbeim, J. Mater Res Soc Proc 2000, 600, 61.
27. Newnham, R. E.; Sundar, V.; Yimnirun, R.; Su, J.; Zhang, Q. M. J Phys Chem B 1997, 101, 10141.
28. Roland, C. M.; Aronson, C. A. Polym Bull 2000, 45, 439.
29. Roland, C. M.; Buckley, G. S. Rubber Chem Technol 1991, 64, 74.
30. Yagi, T.; Teramoto, M.; Sako, J. Polym J 1980, 12, 209.
31. Davis, G. T.; Furukawa, T.; Lovinger, A. J.; Broadhurst, M. G. Macromolecules 1982, 15, 329.
32. Lovinger, A. J.; Davis, G. T.; Furukawa, T.; Broadhurst, M. G. Macromolecules 1982, 15, 323.
33. Lovinger, A. J.; Davis, D. D.; Cais, R. E.; Kometani, J. M. Macromolecules 1988, 21, 78.
34. Forsythe, J. S.; Hill, D. J. T. Prog Polym Sci 2000, 25, 101.
35. Logothetis, A. L. Polym Int 1999, 48, 993.
36. Yoshida, T.; Florin, R. E.; Wall, L. A. J Polym Sci A: Gen Pap 1965, 3, 1685.
37. Mabboux, P. Y.; Gleason, K. K. J Fluorine Chem, 2002, 113, 27.
38. Lovinger, A. J. Macromolecules 1985, 18, 910.
39. Freakley, P. K.; Payne, A. R. Theory and Practice of Engineering with Rubber; Applied Science: London, 1978.
40. Guillot, F. M.; Jarzynski, J. J Acoust Soc Am 2000, 108, 600.
41. Furukawa, T.; Tajitsu, Y.; Zhang, X.; Johnson, G. E. Ferroelectrics 1992, 135, 401.
42. Baltá Calleja, F. J.; González Arche, A.; Ezquerra, T. A.; Santa Cruz, C.; Batallán, F.; Frick, B.; López Carbacos, E. Adv Polym Sci 1993, 108, 1.
43. Menegotto, J.; Ibos, L.; Bernes, A.; Demont, P.; Lacabanne, C. Ferroelectrics 1999, 228, 1.
44. Ferry, J. D. Viscoelastic Properties of Polymers, 3rd ed.; Wiley: New York, 1980.
45. McCrum, N. G.; Read, B. E.; Williams, G. Anelastic and Dielectric Effects in Polymeric Solids; Dover: New York, 1991.